Available online at www.CivileJournal.org

Civil Engineering Journal

Vol. 4, No. 6, June, 2018

Reduced Beam Section (RBS) Moment Connections-Analytical Investigation Using Finite Element Method

Christos E. Sofias [a*], Dimitra C. Tzourmakliotou [b]

[a] *MSc. Civil Engineer, Democritus University of Thrace, Xanthi, 67100, Greece.*

[b] *Associate Professor, Steel Structures Laboratory, Democritus University of Thrace, Xanthi, 67100, Greece.*

Received 8 May 2018; Accepted 26 June 2018

Abstract

Reduced Beam Section (RBS) moment resisting connections are among the most economical and practical rigid steel connections developed in the aftermath of the 1994 Northridge and the 1995 Kobe earthquakes. Although the RBS connection effectiveness was widely investigated using US design and construction practices, only limited data exist from European research. Recommendations of RBS applications in steel frames were prescribed in EC8, Part3. However the reliability of these recommendations is under consideration due to above mentioned poor existing data. This paper examines numerous different contours of radius cut-out (Group A) and provides recommendations for the design and detailing of radius cut Reduced Beam Section (RBS) moment connections. Furthermore, it examines and compares different beam cross sections of European steel profiles (Group B) while the sizing of the RBS cut is kept at a constant ratio. Analytical approach was conducted investigating the adopted by EC8, Part 3 key parameters for the design. The main objective of the applied RBS geometry is to protect the connection and its components (endplate, column flange, bolts, welds) from either plastification or failure. Although the computational cost for optimization with ABAQUS is very large, the results of this study ensures on one hand that the performances of the structural parts can be effectively improved by shape optimization and an the other hand that adjustment in the geometry of the radius cut is needed for safe application to European profiles.

Keywords: Reduced Beam Section Connection; Moment Connection; Extended Endplate Connection; Bolts; Finite Element Analysis.

1. Introduction

Moment Resisting Frames (MRF) design has received particular attention over the last decades. MRF buildings inability to function at the desired response level during the Northridge (U.S.A) and Kobe (Japan) is attributed to early failure of beam to column connections. The unexpectedly serious failures that occurred in these connections, resulting in the inhibition of the plastic hinge at the joints, led to a limited ductility and energy absorption capacity of the connections and thus to the blockage of bending moments redistribution over the MRFs.

* Corresponding author: chsofias@gmail.com

http://dx.doi.org/10.28991/cej-0309170

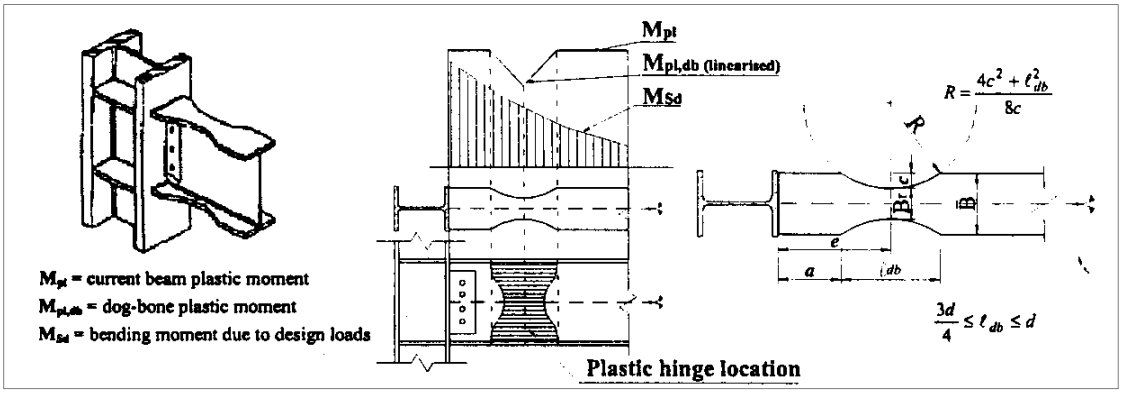

Figure 1. The idea of RBS technique [1, 14 and 15]

An extensive number of experimental and analytical research projects took place after these earthquakes in order to understand the causes of the damage, and to develop improved approaches for these connections to avoid similar damage in future earthquakes [1-4]. Two main strategies have been emerged as the most popular to provide reliable behaviour and ductile response: strengthening the joint (reinforced connections) and /or weakening the frame beam (RBS or dogbone connections [1]), (Figure 1). The first method allows the plastic hinge formation away from the column and the second exploits the beam weakening in an appropriate position away from the steel joint, where plastic deformation occur, with the latter being the most widespread for steel moment frames.

The idea of RBS is based on the beam's flanges cutout in the nearby region of the beam-to column connection. The RBS reduces the moment capacity of the beam at a prescribed distance from the column face and forces the large strains to occur in a more desirable location that can undertake large inelastic deformation, while at the same time it limits the stress development in the less ductile area in front of the column. Various shapes of cut-outs are possible (constant, tapered, or radius) cuts. However, the extensive experimental and analytical research projects carried out shown that the radius cut behaves with the highest rotational capacity and at the same time is relatively easy to fabricate. The RBS design and detailing (geometrical parameters a, b and c) that was suggested by the FEMA 350 [5] and FEMA 351 [6] were adopted in Europe by the EC8, Part 3 [7] and is shown in Table 1.

Several researches were investigating the influence of the RBS technique, most of them including US profiles and type of connections [8, 9 and 10]. Lignos et al. [11] also provided valuable data exported from a large experimental analysis that can describe the RBS response through five damage states. Tsavdaridis et al. investigated the efficiency of beam web impairment (Reduced Web Sections - RWS) providing useful data for steel seismic resistant frames [12]. Furthermore, the T-stub effect and weld access holes existence was studied by Brunesi et al. [13] in seismic response of steel MRF connections. Evaluation of MRF buildings using both RBS and RWS implementations is carried out by Naughton et al. [16]. It is shown that the alternative web impairment has shown well response on buildings up to 8 storeys.

A significant amount of research and testing on RBS moment connections has already been completed using European HEA-profile section providing useful results since so far they have been only investigated by the US design construction practices [14, 15]. Both the experimental results and those of the finite element models reveal the need to readjust the values of the geometrical characteristics of the RBS, so that they can be used safely in bolted moment connections using European section profiles [14]. The aim of this paper is to present a series of simple and accurate three-dimensional (3D) finite element models (FE) capable of predicting the actual behavior of RBS in steel frames subjected to shear loads. The software package ABAQUS [17] is used to model the joint. The bolted extended endplate connection was chosen as an important type of RBS connection due to extensive use in the European section profiles.

2. Finite Element Models

The finite element analysis deals with the investigation of two basic parameters in RBS connection, the type of cross-section and the applied impairment geometry. Moreover, in the analysis for the finite element parametric study the following two applications were examined:

- A series of models using the same beam cross-section, HE180A and with various radius cuts in the RBS connection (both inside and outside the proposed limits according to FEMA [5, 6]), and described in the sequel as "Group A" FEA models. The accurate position and size of the circular cutout has been investigated through numerical modeling, while the plastic hinge positions is effectively controlled.
- A series of models with various cross-section, HEA sizes, and with the same percentage of radius cut area in RBS connection and described in the sequel as "Group B" FEA models.

In order to introduce a reliable FE model, an experimental test carried out using the set-up shown in Figures 2 and 3 [14]. Experimental and analytical results were in satisfactory correlation, meaning that the FE model provides accurate results. The "T" type arrangement was adopted with the impairment geometry as shown in Figure 2. The HEB300 column is of 1797 mm size and the horizontal HEA beam is of 1200 mm. The monotonic shear force was implemented on the HEA beam at 1000 mm away from the column's face developing bending moment at the beam to-column connection and was acting increasingly versus virtual time until failure occurred. Given that the analysis is elastoplastic, loading was imposed by means of displacement (displacement control test), providing higher control level throughout the analysis.

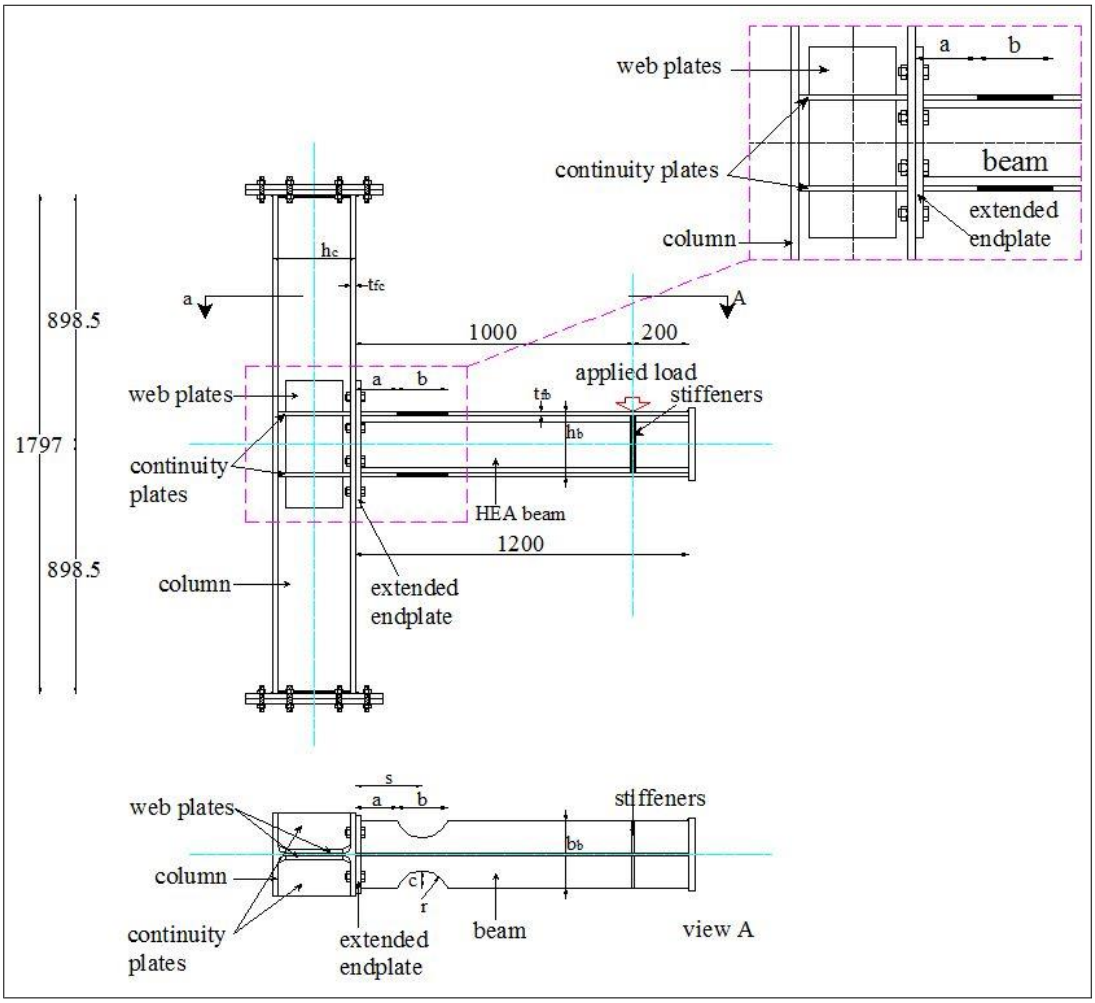

Figure 2. Test set-up [14]

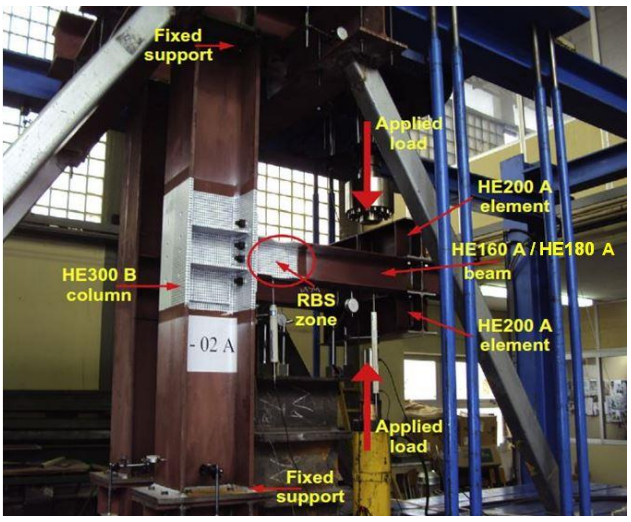

Figure 3. Experimental test set-up [14]

Table 1 provides the applied RBS geometry that was used compared to the FEMA and EC8 recommendations for "Group A" FEA series.

Table 1. Geometric characteristics of RBS cutout ("Group A" FEA models)

	Applied RBS limits	EC8, part 3 limits [7]	FEMA 350 [5] / 351 [6] limits
a	$(0.30 \div 0.90)b_f$	$a = 0.60\ b_f$	$a = (0.50 \div 0.75)\ b_f$
b	$(0.35 \div 1.45)d_b$	$b = 0.75\ d_b$	$b = (0.65 \div 0.85)\ d_b$
c or g	$(0.10 \div 0.30)b_f$	$g \leq 0.25\ b_f$	$c \leq 0.25\ b_f$

In addition, Table 2 helps decoding and understanding code-naming that was given to each of 818 models of "Group A" FEA series, providing the cross-section size of HEA beam and the RBS geometrical parameters ratios. For instance, model HE180A_60/75/25 refers to the model of HE180A beam with respective ratio values of a=0.60, b=0.75 and g (or c)=0.25.

Table 2. Code-naming of Finite Element Models ("Group A" FEA models)

Row	**1**	**2**	**3**	**4**
Value	**180**	**30 to 90**	**35 to 145**	**10 to 30**
Incrementation step	**-**	**5**	**10**	**2.5**
1	Beam cross-section type			
2	RBS parameter **a**			
3	RBS parameter **b**			
4	RBS parameter **g** or **c**			

The efficiency of five (5) different HEA cross-section for the RBS connection is examined in "Group B" FEA. Table 3 shows the different HEA cross sections together with the extended plate, the type and the grade of bolts. Table 4 shows the geometry of the circular cuts used in each one of the five HEA sections. In this table it can be seen that the circular cutouts maintained a constant ratio for each one of the models under investigation. The extended endplate connection was chosen for Group B since is one the most commonly used in steel moment resistant frames in Europe.

Table 3. Extended endplate connection definition ("Group B" FEA models)

Column cross-section	Beam cross-section	Extended endplate	Steel grade	Bolts grade
HE300B	HE160A	310 x 200 x 20	S 275	M 20 8.8
HE300B	HE180A	350 x 200 x 20	S 275	M 24 10.9
HE300B	HE200A	350 x 200 x 20	S 275	M 24 10.9
HE300B	HE220A	390 x 220 x 20	S 275	M 24 10.9
HE300B	HE240A	390 x 240 x 25	S 275	M 24 10.9

Table 4. RBS geometry application ("Group B" FEA models)

Beam cross-section	b_f	d_b	a		b		g		s	r
	(mm)	(mm)	$\%b_f$	(mm)	$\%d_b$	(mm)	$\%b_f$	(mm)	(mm)	(mm)
HE160A	160	152	70	112	75	114	40	32	169	66.7
HE180A	180	171	70	126	75	128	40	36	190	75.1
HE200A	200	190	70	140	75	143	40	40	211.2	83.4
HE220A	220	210	70	154	75	158	40	44	232.7	92.4
HE240A	240	230	70	168	75	173	40	48	254.2	101.5

By taking advantage of model's symmetry through the transverse axis, the size of the analysis domain can be reduced. This reduction in analysis domain would reduce substantially the computational time without affecting the accuracy of the results. The numerical model developed in ABAQUS [17] consists of sub-assemblages of a column and a beam connected to each other by means of an endplate welded to the beam and bolted to the column flange and are representative of an external node of a moment resisting framed structure with extended endplate joints. The lengths of the beam and the column are established according to the experimental tests setup used in the validation of the FE models. Correct representations of the boundary conditions are essential since slightly different boundary conditions can produce significantly different results. For the simulation in this paper, the boundary conditions were taken as being exactly the same as in the tests as shown in Figure 4. Specifically, both column's ends were fixed (areas 1 and 2) and in addition, boundary conditions at the symmetry level were imposed.

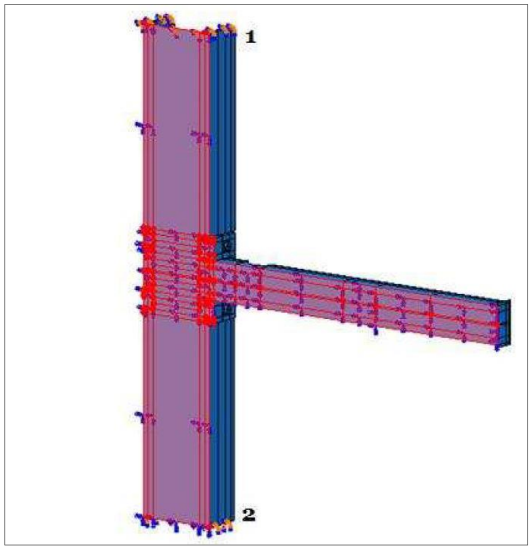

Figure 4. FEM boundary conditions at fixed points 1 & 2 (head and base of the column) and at symmetry on the transverse axis

The models are composed of volumetric C3D8R (8 nodes and 3 degrees of freedom per node – element from the ABAQUS Library) finite elements in the joint region i.e. the column flanges, extended endplate, bolts and nuts. Four-node S4R shell elements (two-dimensional elements with thickness definition - 4 nodes and 6 degrees of freedom per node-element from the ABAQUS Library) were used to simulate the beam, and the column segments, aiming at reducing the computational time. This option emerged after a repetitive sequential testing process where initially all parts of the model were simulated with volumetric elements C3D8R. Due to the existence of the bolts, it was not possible to simulate all parts with shell elements except those that were not in contact with the bolts. Figure 5 illustrates, by means of a graphical representation, the above distinction of each part that composes the analytical model, as well as the denser element grid applied to the area of both the endplate connection and the RBS which are the areas of greater interest. Moreover, the FE model has the ability to be modified easily and then resolved repeatedly to take the different geometric and material parameters that affect the behavior of RBS connection into account and in accordance with the requirement of Group A and Group B cases as stated previously.

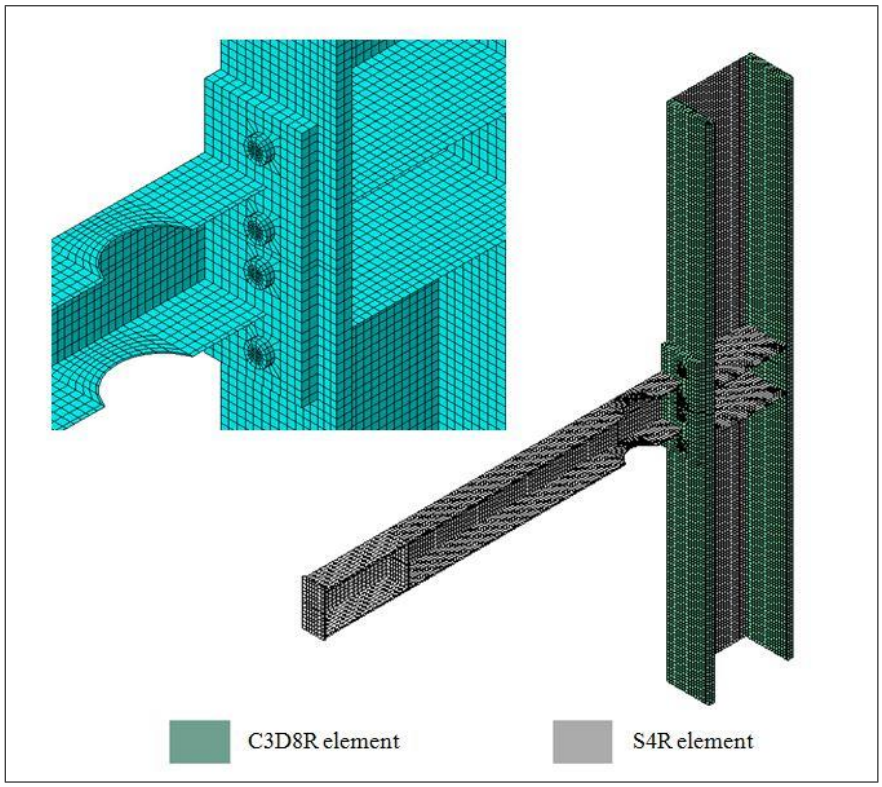

Figure 5. Finite Element Design

3. Finite Element Analysis Results

As previously mentioned, Finite Element Analysis simulation is divided in two distinct work phases where the behaviour of beam to column moment connection under monotonic loading is studied. The connection is implemented with extended endplate where the RBS technique is applied. Post-elastic response is evaluated, whether the applied RBS circular beam flange cutout can protect the beam to column connection, providing at the same time better ductility level. A critical objective of this investigation, is the assessment of the RBS recommendations foreseen in EC8-Part 3, in which case the geometric parameters a, b and g (or c) that has been implemented were inside and outside the recommended limits ("Group A" FEA models). Finally the influence of the beam's cross-section size using the same RBS geometry is investigated ("Group B" FEA models).

3.1. "Group A" FEA Models

In this paragraph, force-displacement (P-δ) and moment-rotation (M-φ) diagrams are shown. As in Group A were examined 1404 analytical FEA models is not possible to present the relevant diagrams for each one of those models. Therefore, it is chosen to include only the representative visual illustration of model behavior. Hence, results from RBS application within and outside the recommended limits [5, 6, 7] are provided. A model without RBS application is also included in the diagrams in order to evaluate better the results of the FE analysis. Furthermore, Figures 6 and 7 provide illustrations from the finite element analysis for the visual evaluation on the behavior of the models. The appearance or absence of the plastic hinge at the desired position on the RBS area (grey-color contour) of the beam are also shown in these figures.

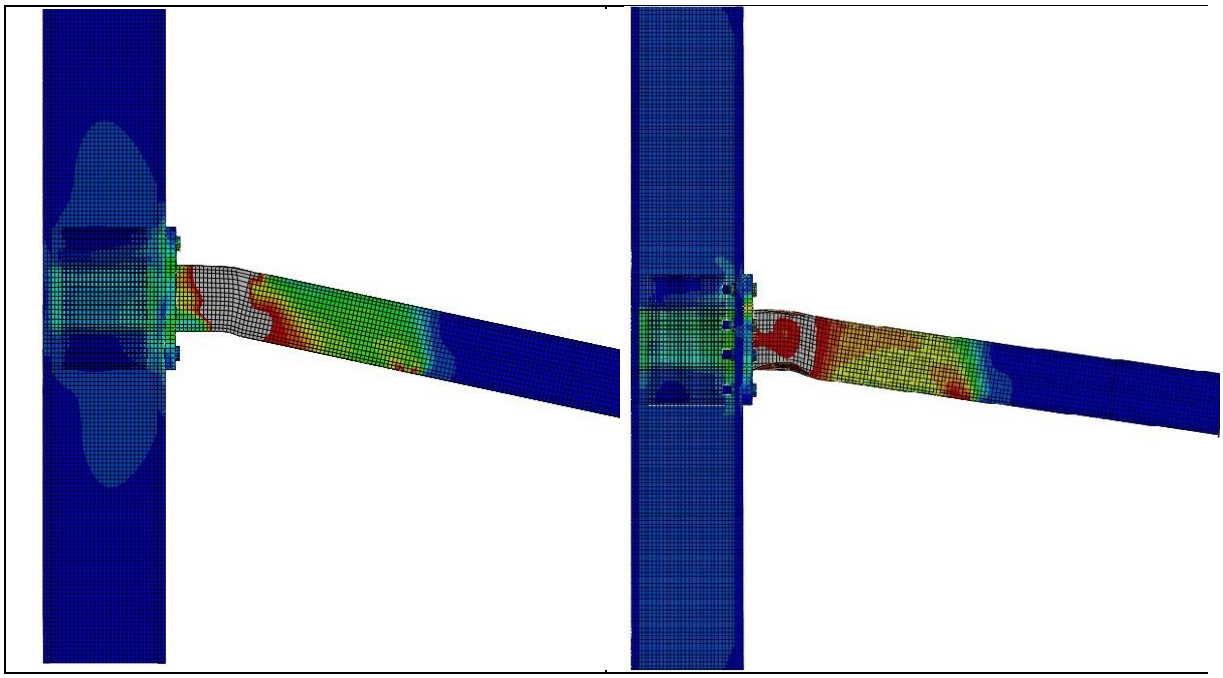

Figure 6. Behavior of representative FEA models (left - HE180A_60/75/25 & right HE180A_45/75/20)

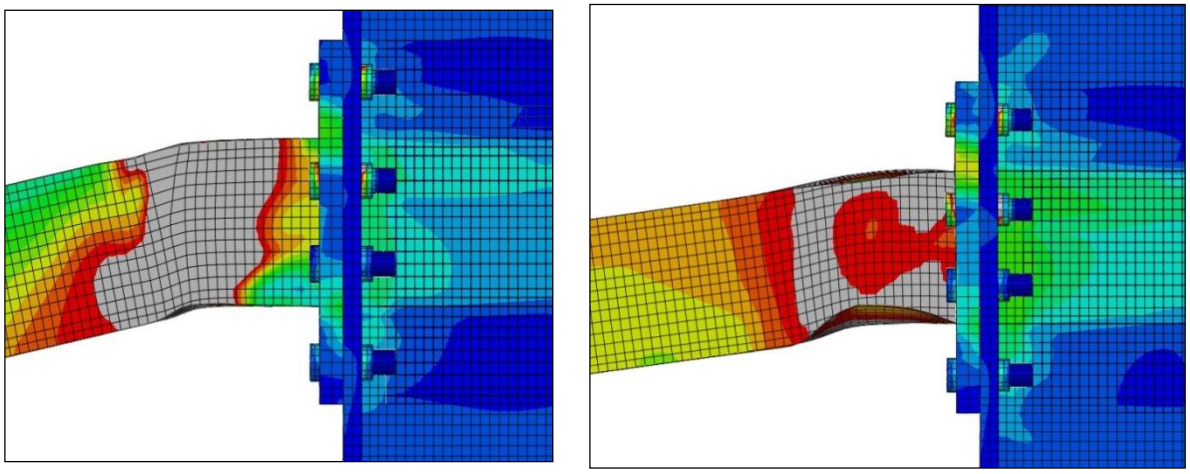

Figure 7. Plastic hinge formation (grey area) of representative FEA models (left - HE180A_60/75/25 & right HE180A_45/75/20)

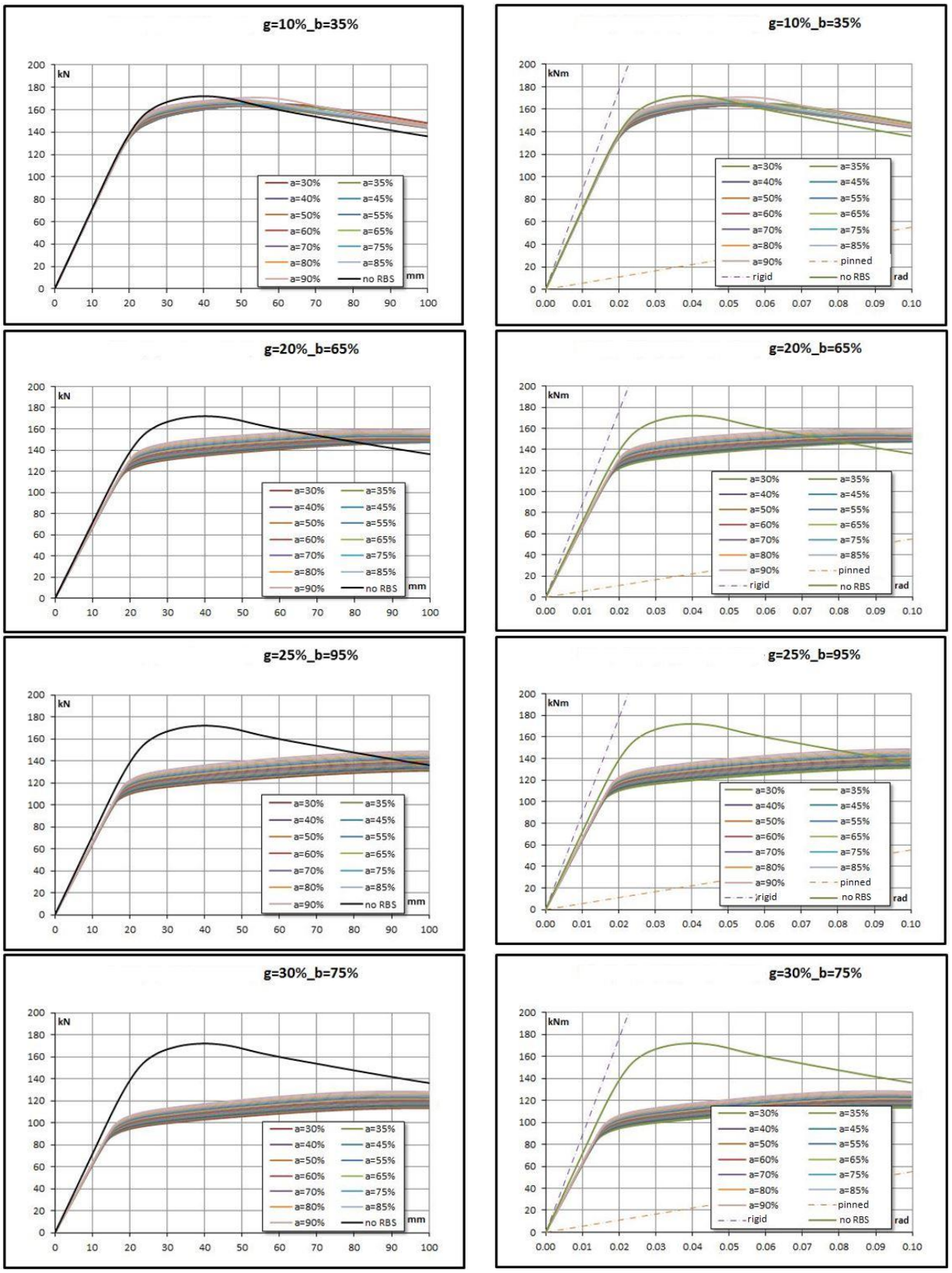

Figure 8. Representative diagrams P-δ (left) & M-φ (right).

3.2. "Group B" FEA Models

"Group B" deals with the variation of cross section of the HEA beam and its influence on the RBS efficiency is investigated. "Group B" FEA models examine different HEA sizes namely, HE160A, HE180A, HE200A, HEA220 and HE240A, with the corresponding extended endplate bolted connection. The RBS geometry was kept at a constant ratio for each one of the models. Moment-rotation (M-φ) diagrams for each one of the above mentioned HEA models are shown in Figures 9, 13, 17, 21, 25 accordingly, in Figures 10-12, 14-16, 18-20, 22-24 and 26-28 illustrations of the connection and RBS are given.

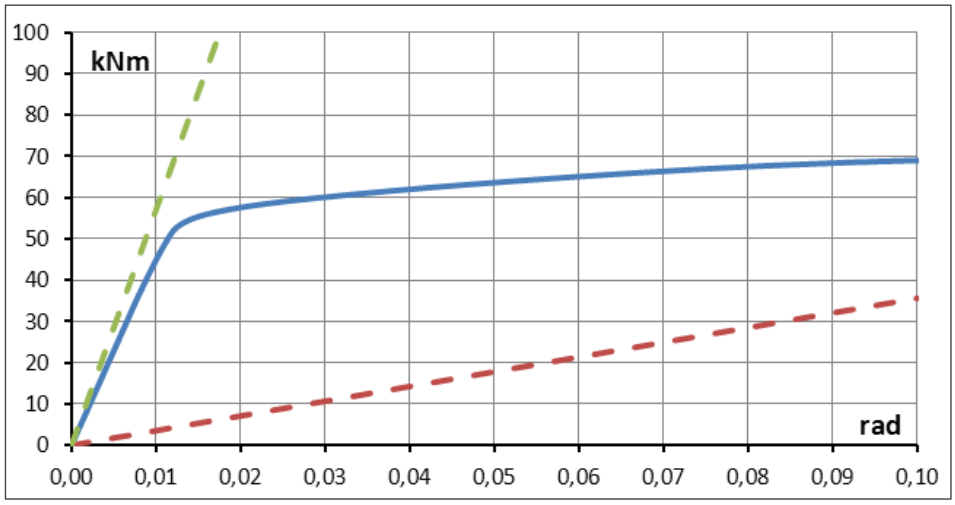

Figure 9. M-φ diagram for HE160A FEA model

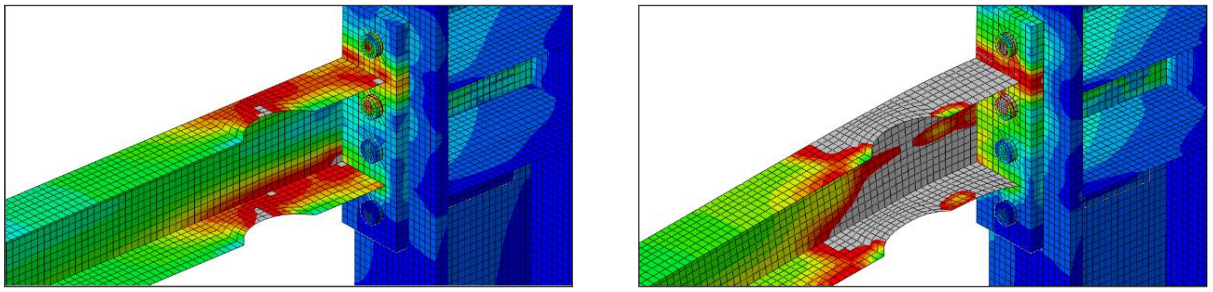

(α) **(b)**

Figure 10. Yield growth at the RBS center (α) and plastic hinge formation (b) - HE160A

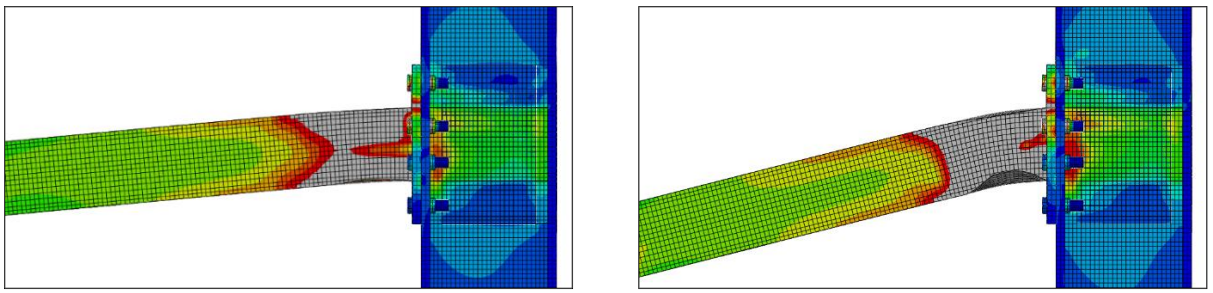

(α) **(b)**

Figure 11. Model view when yield occurs (α) and final beam deflection (b) - HE160A

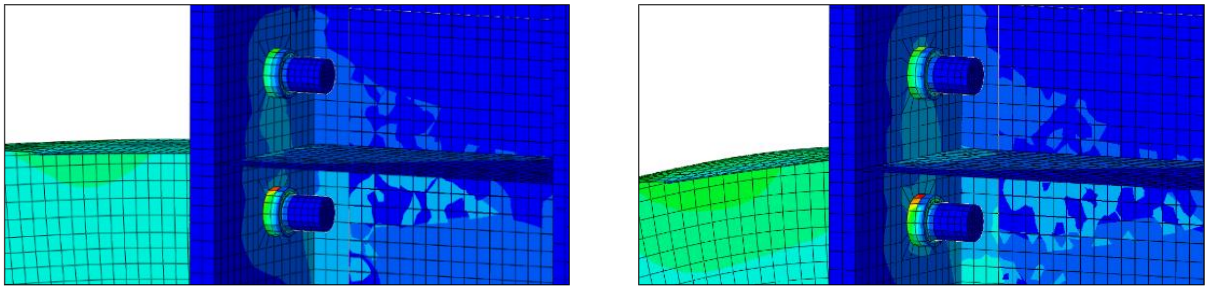

(α) **(b)**

Figure 12. Stress development over the bolts when plastic hinge formation occurs (α) and at the final loading stage (b) - HE160A

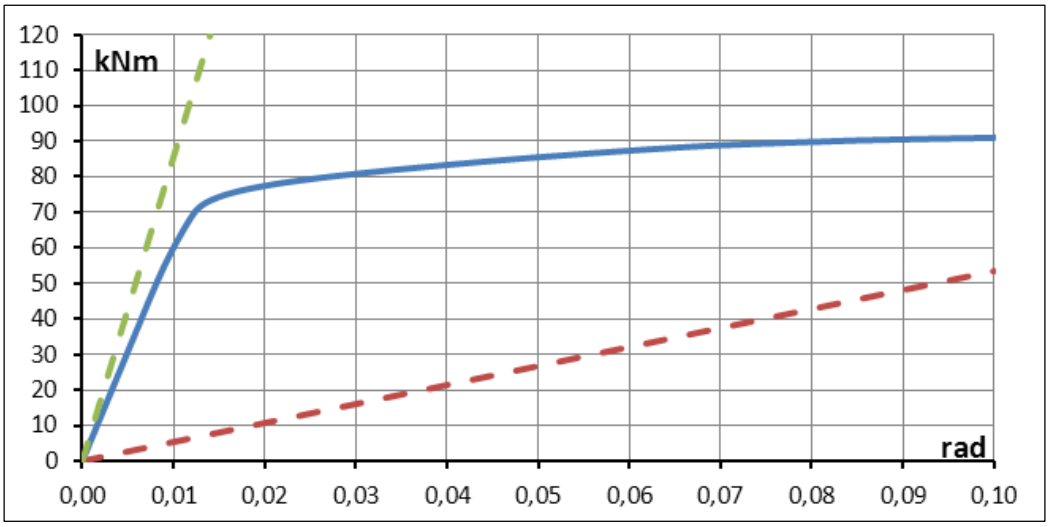

Figure 13. M-φ diagram for HE180A FEA model

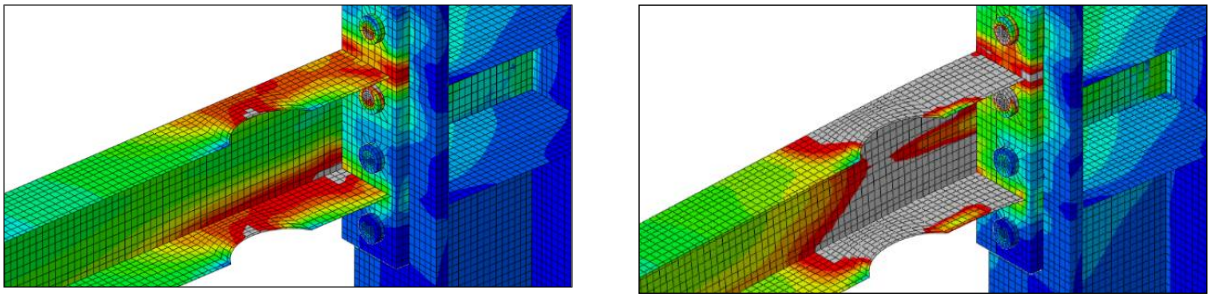

(α) **(b)**

Figure 14. Yield growth at the RBS center (α) and plastic hinge formation (b) - HE180A

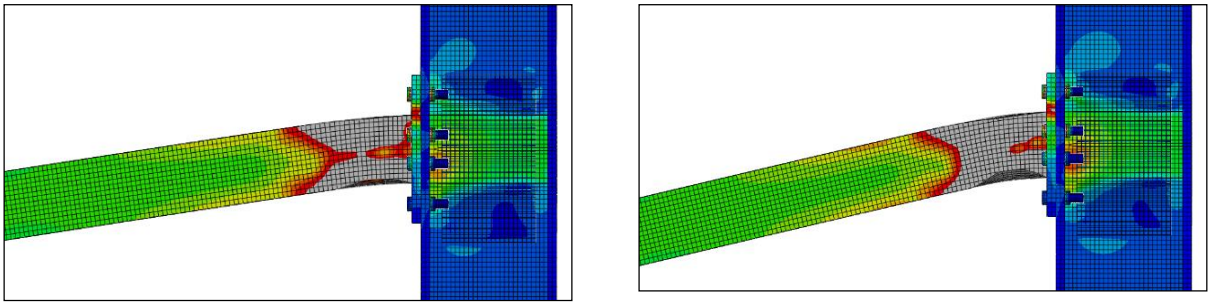

(α) **(b)**

Figure 15. Model view when yield occurs (α) and final beam deflection (b) - HE180A.

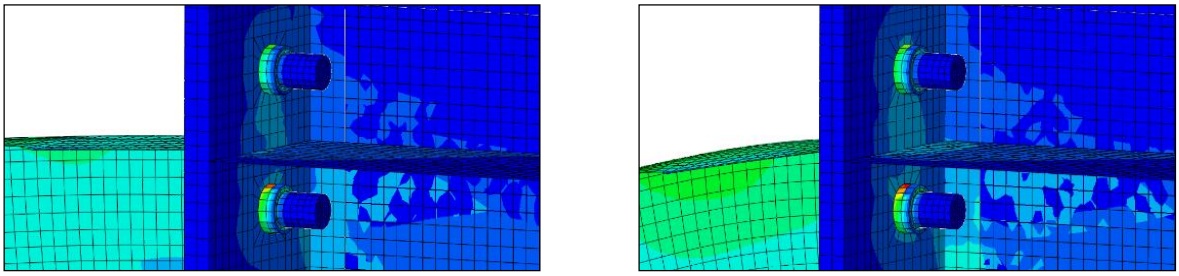

(α) **(b)**

Figure 16. Stress development over the bolts when plastic hinge formation occurs (α) and at the final loading stage (b) - HE180A

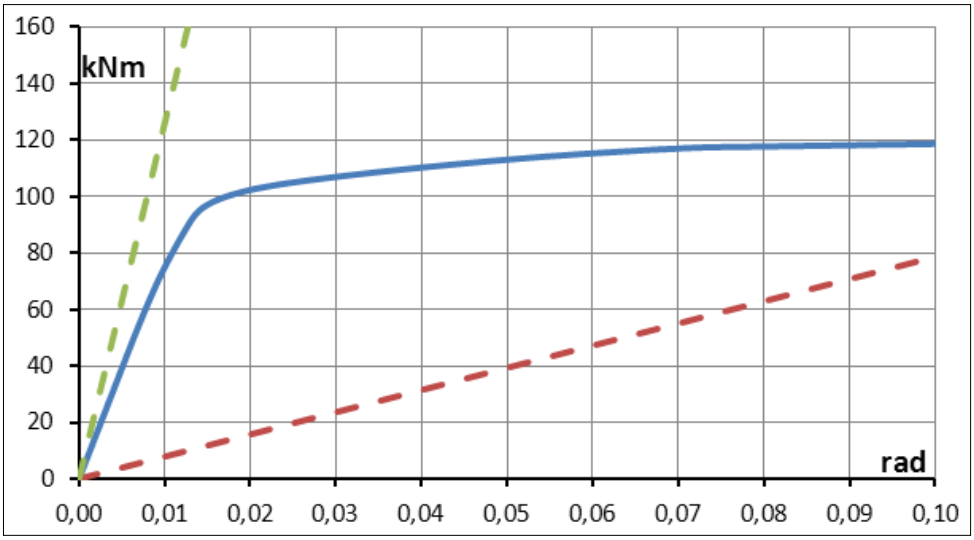

Figure 17. M-φ diagram for HE200A FEA model

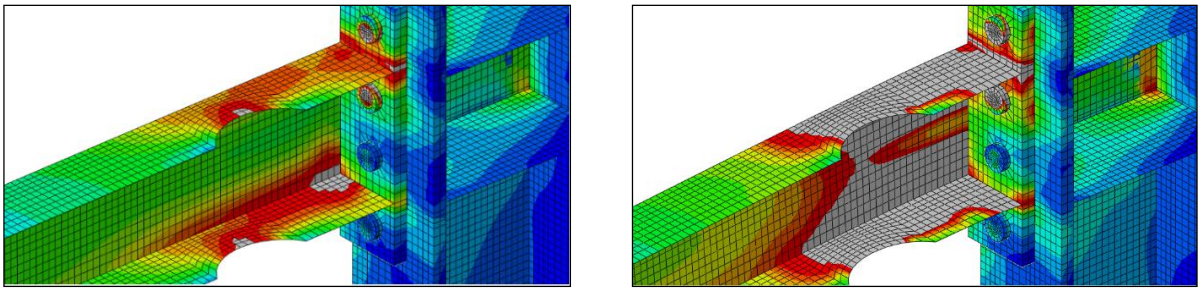

(α) **(b)**

Figure 18. Yield growth at the RBS center (α) and plastic hinge formation (b) - HE200A

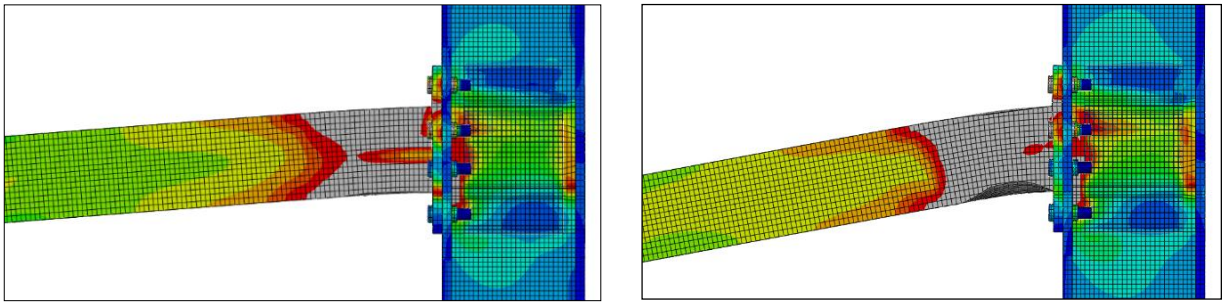

(α) **(b)**

Figure 19. Model view when yield occurs (α) and final beam deflection (b) - HE200A

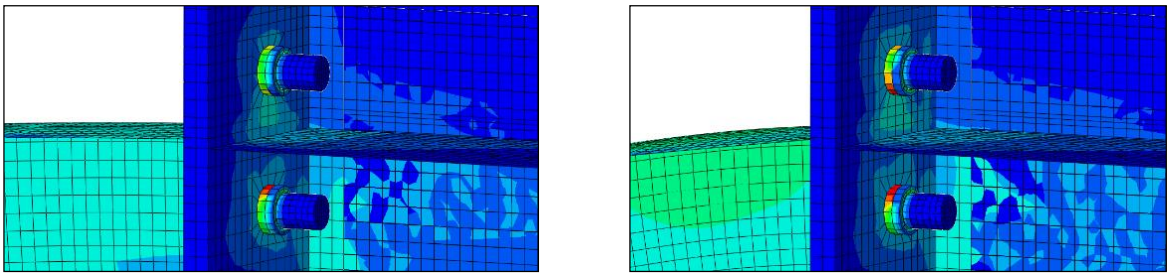

(α) **(b)**

Figure 20. Stress development over the bolts when plastic hinge formation occurs (α) and at the final loading stage (b) - HE200A

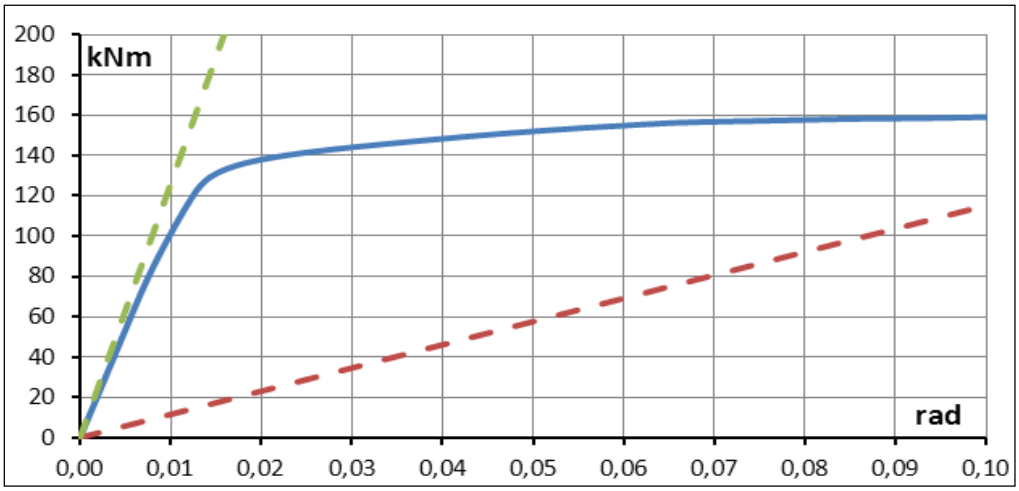

Figure 21. M-φ diagram for HE220A FEA model

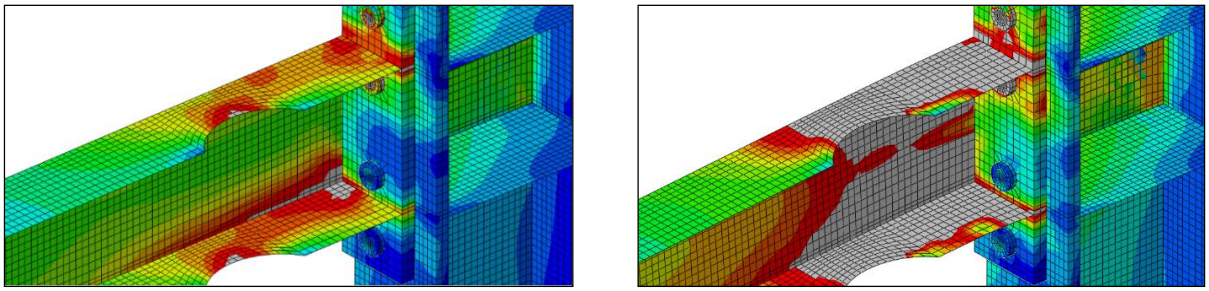

(α) **(b)**

Figure 22. Yield growth at the RBS center (α) and plastic hinge formation (b) - HE220A.

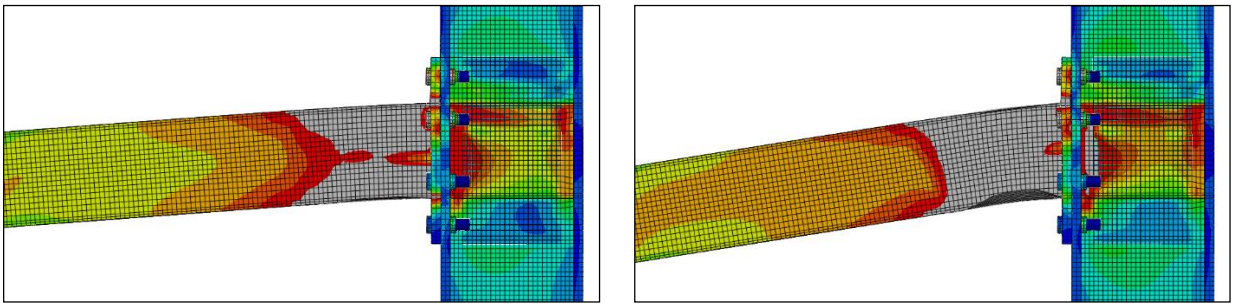

(α) **(b)**

Figure 23. Model view when yield occurs (α) and final beam deflection (b) - HE220A

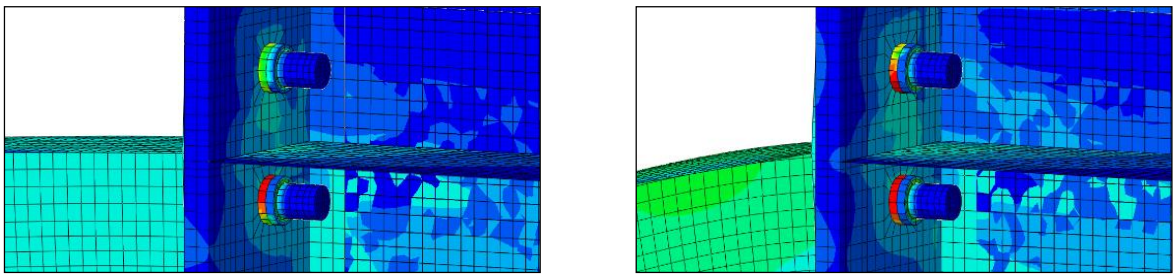

(α) **(b)**

Figure 24. Stress development over the bolts when plastic hinge formation occurs (α) and at the final loading stage (b) - HE220A

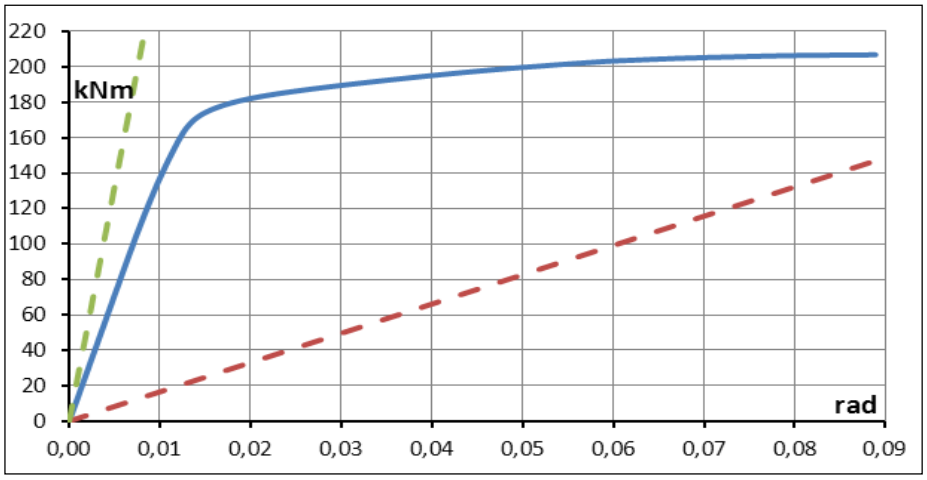

Figure 25. M-φ diagram for HE240A FEA model

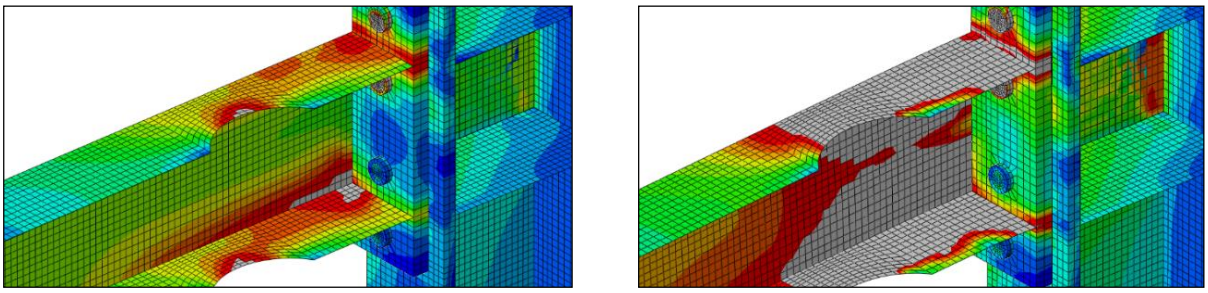

(α) **(b)**

Figure 26. Yield growth at the RBS center (α) and plastic hinge formation (b) - HE240A

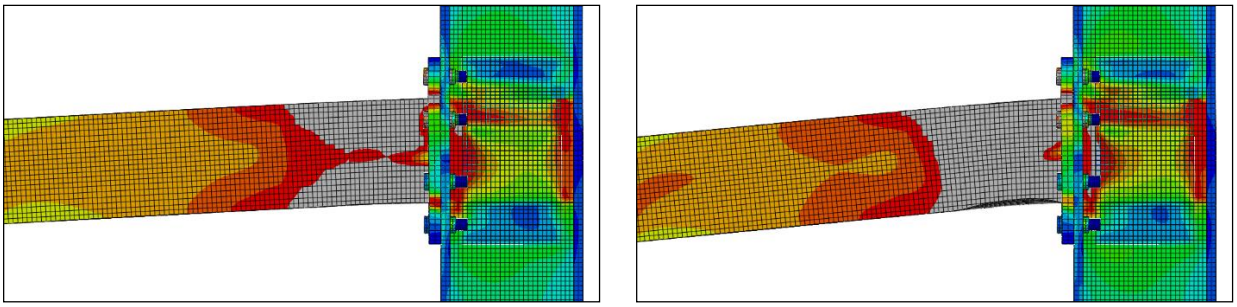

(α) **(b)**

Figure 27. Model view when yield occurs (α) and final beam deflection (b) - HE240A

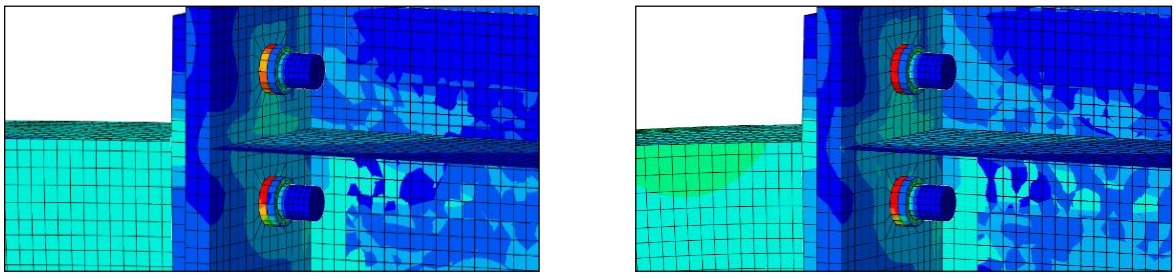

(α) **(b)**

Figure 28. Stress development over the bolts when plastic hinge formation occurs (α) and at the final loading stage (b) - HE240A

4. Conclusion

This paper presents a comprehensive FE parametric study introducing:

- RBS with different circular cutout and extended endplate bolted connections ("Group A" FEA
- HEA beams with five different cross sections and circular cutout with constant ratio of geometric parameters ("Group B" FEA models),

Subjected to monotonic loading. It is essential for the connection to be sufficiently strong and robust, mobilizing the stresses to a desired location along the length of the beam away from the connection assembly, creating the "weak beam-strong column" mechanism through the formation of plastic hinges proving the performance of RBS connections with European section HEA beams to be used in seismic resistant designs.

It is concluded from the results of "Group A" that such connections behave in a satisfactory manner and provide an ideal structural behavior in terms of stress distribution, especially when the corresponding beam can form the plastic hinge in the impairment area. In such case, the beam to column connection remains in the elastic area and the connection parts (extended endplate, bolts, nuts and welds) are protected from any form of failure. The Parametric Finite Element Analysis demonstrates that the successful RBS application is ensured when the values of the geometric parameters of the impairment follow specific geometric combinations.

These values are placed either within or outside the recommended limits, as set at the existing regulations (FEMA 350/351 and EC8-Part3). However, the study showed combinations of values that although they are within the above limits, do not ensure the plastic hinge formation in the intended area. Therefore, this study contributes a huge amount of data on safe RBS application using European cross section profiles for beam to column moment connections. An ongoing research forms a catalogue of successful combinations of geometric values of RBS application for European cross section profiles. Table 5 provides indicative suggestions for geometrical parameters combinations, where the plastic hinge formation occurs in the desired area.

Table 5. Values of a and b geometrical parameters for radius cut of c (or g) = 0.15÷0.175 for successful RBS application

RBS parameter	a	b	c or (g)
combinations	0.30÷0.45	0.65÷0.75	0.15
	0.30÷0.50	0.85	0.15
	0.30÷0.65	0.95	0.15
	0.30÷0.40	0.50	0.175
	0.30÷0.45	0.60÷0.70	0.175
	0.30÷0.55	0.80	0.175
	0.30÷0.60	0.90÷1.00	0.175

Table5: Values of a and b geometrical parameters for radius cut of *c (or g) = 0.15÷0.175* for successful RBS application.

Is derived from the carried out analysis of "Group B" that the cross section size is a critical parameter for the successful RBS application. Continuing to analyze the results of "Group B" turns out that by increasing the stiffness of the beam, through the height of the cross-section, the application of the same circular cutout leads to a decrease in the influence of the technique on the protection of the connection. For HE160A and HE180A beams the RBS application leads the plastic hinge formation in the center of the cutout area, resulting to the protection of the beam to column connection.

Even though similar behavior occurs on the HE200A beam an increased deformation level of the endplate is noted in parallel. As far as HE220A and HE240A sections concern is derived from this study that the RBS application is not that efficient as for the aforementioned sections since it is no longer clear that the use of circular cutout contributes to the protection of the joint. Moreover, large deformation is noted in the endplate and increased stress growth evolves on the bolts since the plastic hinge never appears in the desired area of the cutout.

5. Nomenclature

RBS	Reduced Beam Section
a	Distance of the beginning of the RBS from the column face
b	Length of the RBS
bf	Flange width
db	Beam depth
E	Modulus of elasticity
fy	yield strength

fu	Ultimate strength
G	Shear modulus
g	Depth of the flange cut
l	The distance between load axis and the column face axis
M	Bending moment
M-φ	Moment vs. rotation
P	Load
P- δ	Load vs. displacement
r	Radius of the cuts in both top and bottom flanges at the RBS
s	Distance of the intended plastic hinge at the centre of the RBS from the column face
ti	Thickness of element i
δy	Displacement at yield point
ν	Poisson's ratio in elastic stage
φ	Rotation of the joint

6. References

[1] Plumier A. Behaviour of connections. J. Construct. Steel Research 1994; 29: 95-119. https://doi.org/10.1016/0143-974x(94)90058-2.

[2] Chen SJ, Chu JM, Chou ZL. Dynamic behavior of steel frames with beam flanges shaved around connection. J. Construct. Steel Research 1997; 42 (1): 49-70. https://doi.org/10.1016/s0143-974x(97)00011-4.

[3] Engelhardt MD, Sabol TA. Seismic-resistant steel moment connections: developments since the 1994 Northridge earthquake. In: Zandonini R, Elnashai A, Dexter R, Editors. Progress in structural engineering and materials; 1997; 1(1): 68-77. https://doi.org/10.1002/pse.2260010112.

[4] Popov E, Blondet M, Stepanov L. Application of dog bones for improvement of seismic behavior of steel connections. Report No UCB/EERC 96/05 1996, U.S.A.

[5] FEMA 350. Recommended seismic design criteria for new steel moment-frame buildings. Washington D.C., 2000.

[6] FEMA 351. Recommended seismic evaluation and upgrade criteria for existing welded steel moment frame buildings. Washington D.C., 2000.

[7] EC 8, Part 3: Design of structures for earthquake resistance. Assessment and retrofitting of buildings. EN 1998-3: June 2005E.

[8] Adan SM, Reaveley LD. The reduced beam section moment connection without continuity plates. In: Proc. Of 13th World Conference on Earthquake Engineering (13 WCCE), Vancouver, Canada; 2004.

[9] Deylamy A, Moslehi Tabar A. Experimental study on the key issues affecting cyclic behaviour of reduced beam section moment connections. In: Proc. Of 14th World Conference on Earthquake Engineering (14 WCCE), Beijing, China; 2008.

[10] Moon K-H, Kim B-Ch, Hwang S-H, Han SW. Seismic performance evaluation of the steel moment frames with reduced beam section connections with bolted webs. In: Proc. of 5th International Symposium on Steel Structures, Seoul, Korea; 2009.

[11] Lignos D, Kolios D, Miranda E. Fragility assessment of reduced beam section moment connections. J Struct Eng 2010;136(9):1140–50. https://doi.org/10.1061/(asce)st.1943-541x.0000214.

[12] Tsavdaridis, K. D., Faghih, F., and Nikitas, N. Assessment of perforated steel beam-to-column connections subjected to cyclic loading. J. Earthq. Eng. 2014; 18, 1302–1325. https://doi.org/10.1080/13632469.2014.935834.

[13] Brunesi E., Nascimbene R., Rassati G.A. Seismic response of MRFs with partially-restrained bolted beam-to-column connections through FE analyses. J. of Contructural Steel Research 2015; 107: 37-49. https://doi.org/10.1016/j.jcsr.2014.12.022.

[14] Sofias, C. E., Kalfas, C. N., and Pachoumis, D. T. Experimental and FEM analysis of reduced beam section endplate connections under cyclic loading. J. Engineering Structures 2014; 59: 320–329. https://doi.org/10.1016/j.engstruct.2013.11.010.

[15] Pachoumis DT, Galousis EG, Kalfas CN, Efthimiou IZ. Cyclic performance of steel moment-resisting connections-experimental analysis and finite element model simulation, J. Engineering Structures 2010; 32: 2683-2692. ttps://doi.org/10.1016/j.engstruct.2010.04.038.

[16] Naughton D.T., Tsavdaridis, K.D. Maraveas C., Nicolaou A., Pushover Analysis of Steel Seismic Resistant Frames with Reduced Web Section and Reduced Beam Section Connections. Frontiers in Built Environment, Vol. 3, Oct. 2017. https://doi.org/10.3389/fbuil.2017.00059.

[17] ABAQUS/PRE. Users manual. Hibbit, Karlsson and Sorensen Inc., 1997.